TWO DIFFERENT STOCHASTIC APPROACHES MODELLING THE DECAY PROCESS OF MASONRY SURFACES OVER TIME

E. Garavaglia[1], B. Lubelli[1], L. Binda[1]

Abstract

Masonry structures subjected to aggressive environment may suffer degradation during their service life; the decay strongly depends on type of the component materials and the technique of construction. This can lead the structure to high states of damage even if not failure. The great randomness connected with the occurrence of critical attacks suggests approaching the deterioration process of masonry under a probabilistic point of view. Following this way, the deterioration process L(t) of stone masonries has been carried out. It has been approached as:

1) *L(t) time dependent stochastic process of the random variable (r.v.)* ℓ.
2) *L(t) time dependent stochastic process of the r.v.* τ.

The approaches 1) and 2) are able to model the reliability of masonry materials over time and predict, in probabilistic terms, the occurrence time of the expected damage.

The procedures have been applied to full-scale models built in Milan in 1990. To measure the masonry decay in time a non-destructive technique has been adopted and the data collected have been elaborated using the approaches 1) and 2). The results obtained allow the good convergence of both the procedures as well as their different possible applications. On the base of these results a discussion on the possible use of these procedures in the maintenance strategies planning is introduced.

Key Words: Environmental Attacks, Deterioration of Building Materials, Salt Crystallisation, Stochastic Processes, Fragility Curves, Renewal Theory.

---

[1] Department of Structural Engineering, Polytechnic of Milan, Piazza L. da Vinci 32, I-20133 Milano, Italy

Résumé

Les structures en maçonnerie soumises à un environnement agressif peuvent subir des dégradations pendant leur temps de vie. Ce dégradations dépendent beaucoup des types de composant utilisés et de la technique de construction. Cela peut amener la structure à de grave dommage jusqu'au collapsus total. La multiplicité et la causalité des paramètres impliqués au cours de ces événements critiques, suggèrent de aborder le processos de dégradation de la maçonnerie avec une approche probabiliste. Le processos de dégradation L(t) de maçonneries en pierre a donc été étudié selon cette approche. Les dommages ont été considéré comme:

1) *L(t) stochastique dépendant du temps selon la variable aléatoire (r.v.)* ℓ

2) *L(t) stochastique dépendant de la variable (r.v)* τ.

Cette approchs nous permettent de modéliser la fiabilité des composants de la maçonnerie dans le temps et de prévoir probabilistiquement, le moment où surgiront les dommages. Les procédures ont été appliquées sur des modèles grandeur nature construits à Milan en 1990. Pour mesurer l'état de dégradation de la maçonnerie dans le temps, une technique de monitorage non destructive a été employées et les données obtenues ont été élaboré selon les approches 1) et 2). Les résultats montrent et une possible convergence des deux procédures et leurs différentes applications. Sur la base des résultats on propose une discussion sur un possible usage de ces procédures dans la planification des interventions de maintenance.

1. Introduction

Masonries subjected to aggressive environment may suffer degradation during their service life. The knowledge of the deterioration processes and of their causes is needed in order to choose the most appropriate types of repair and protection. The experience shows that, in the Mediterranean countries where the freezing and thawing action is not present or not severe, the most important cause of damage is salt crystallisation. The moisture present in the wall, due to capillary rise and/or rain penetration, is the vehicle through which soluble salts are distributed inside the material. The evaporation process takes place towards the external surface of the walls; salts crystallising behind the surface cause delamination and crumbling of the masonry components.

In order to investigate the effects of the aggressive environments on masonry, some full-scale stone models were built in a polluted area of Milan. Since 1990 they were subjected to capillary rise and salt attacks and the surface damage was monitored through a non-destructive laser device [1, 2]. The characteristics of the outdoor model and of the decay test procedure are described in Section 2.

The great randomness connected to the occurrence of critical environment suggests studying the deterioration of the masonry and of the building materials under a probabilistic point of view [3, 4 and 5].

Following this way, the analysis of the deterioration process, occurring in a real wall when subjected to aggressive environment, has been carried out applying two different stochastic approaches:

1. The deterioration process $L(t,\ell)$ over time defined as a stochastic process of the random variable (r.v.) ℓ, where ℓ is the loss of surface material [6]
2. The deterioration process $L(t)$ over time defined as a stochastic process of the r.v. τ, where τ is the "lifetime" of the system [7].

The theoretical aspect of these approaches is presented in Section 3.

In Section 4 the results obtained by the application of the two approaches are reported; furthermore a comparison between these two approaches is presented and a discussion on the possible use of these procedures in the maintenance strategies planning is introduced.

A summary of results is given in Section 5, which includes some closing remarks.

2. Experimental tests

2.1 Full-scale models description

The on-site research was carried out on three full-scale models built, in a polluted area of Milan, in 1990 by L. Binda and G. Baronio in collaboration with ICITE-CNR, S. Giuliano M. and ESEM, Milan. Some panels of the models were treated in 1992, others in 1996.

The geometry and exposure of the model were designed to obtain the fastest decay in a natural environment in both the treated and untreated cases. Therefore, a continuous capillary rise of water inside the walls was realised together with the possibility of producing an accelerated decay due to salt crystallisation [1 and 2].

Two types of materials were chosen: (1) soft mud facing bricks used for restoration of historic buildings; (2) sandstone called "Pietra Serena" coming from Toscana, and largely used in the central part of Italy. Putty lime and siliceous sand in the proportion of 1:3 composed the mortar chosen for all the masonries.

The models are one-storey constructions with the facades divided into modular orthogonal panels exposed south and west (Fig.1a and 1b). Two models: one with sandstone (named model A) and one with soft mud facing brick (named B) have five pairs of orthogonal panels each (named respectively A1 to A5 and B1 to B5) (Fig. 1a). The third model (named C), with mixed stone and brick (C1 to C4), has only four pairs of orthogonal panels (Fig. 1a). The construction of the models ended on September 1990.

In order to study the effect of salt crystallisation, an artificial decay is caused in some areas of bottom of the walls. The subsoil of the structures was excavated to a certain level and the foundation soil was coated with a layer of bentonite in order to avoid drenage of the soil.

2.2 Environmental monitoring system

The continuous monitoring of environmental data (temperature and R.H. of the air, temperature of the surface of the walls, water level in sub soil) began in 1990.

The main aim of this survey is to find a correlation between the environmental data and the other variables that are involved in the damage process, i.e. presence of water in the masonry and consequently salt crystallisation and freezing and thawing action.

The presence of water in the subsoil is controlled by five piezometers. The monitoring system of the environmental data (Fig. 2a) is composed by:

- 8 hygrothermometers for the measure of the temperature and R.H. of the air, inside and outside the models;
- 1 cupped tacho-anemometer that collects data on the wind speed;
- 1 pyranometer that measure sun radiation;
- 36 thermocouples that survey the temperature on the internal and external, upper and lower, surface of the walls.

All the data are collected and recorded by a data-logger.

2.3 Recording and elaboration of the data

The effect of decay due to salt crystallisation in masonry walls is a continuous crumbling and delamination of the external surface of the wall while the inside is left unaltered. For this reason the variation in roughness of the surface can be considered a measure of the damage occurred to the masonry.

The authors in [8] proposed for the first time a measurement procedure of the surface decay. The device used is a laser profilometer described by the authors in [2] and [9] (Fig.2b).

The device, of which the schema is shown in Figure 2c, allows to draw vertical profiles of the wall in the chosen positions (Fig. 3).

Subsequent measurements show how the profile is changing in time due to any superficial decay caused by freeze-thaw, salt crystallisation, air pollution, etc.

In this way it is possible to measure the material loss in time and to assume it as a parameter of damage for the wall. The Fig. 4a shows an example of profiles corresponding to the six different measurements carried out from 1993 to 1998.

On the basis of the laser profilographer plots, the difference between the co-ordinates of the same points, detected within subsequent measurements, allows the loss of material to be calculated. Bulging of the profile at a certain measurement indicates the initial detachment of a surface layer, which in turn is followed by a sudden reduction in profile when the layer drops off (Fig. 4b). The presence of swelling phenomena could compromise the damage measurements. Nevertheless since bulging is a first step before detachment, it is possible to consider it as the starting point of damage. Under this consideration a simple computer code has been studied to convert the experimental diagrams (Fig. 4) into modified diagrams where bulging has been removed (Fig. 5) [6].

The procedure carries out the comparison between the horizontal co-ordinates of two subsequent diagrams: the current plot *n* and the previous plot $(n-1)$. Usually the co-ordinates of the diagram *n* are smaller than the ones of the diagram $(n-1)$, except for the points affected by swelling. In these points the computer code continues the procedure comparing the co-ordinates of the plot *n* with the ones of the successive plots $(n+1)$, $(n+2)$, $(n+3)\ldots$ until a plot m=(n+i) having smaller horizontal values than the ones of the profile *n* is found. The co-ordinates of the diagram *m*, corresponding to the points affected by bulging, become the new reference co-ordinates of profile *n* when it will be remade. As a result, a clean plot of the evolution of the surface damage as a function of time and space has been obtained (Fig.5).

In order to quantify the damage of the wall as “the loss of the cross section of the wall with time”, the area ΔA_i between two consecutive diagrams of Figure 5 (ΔA_i = the dashed area in Figure 5) has been assumed as a parameter. This area is automatically calculated within the assumed computer code [6].

In order to quantify the evolution of the loss of the cross section over time, for each profile shown in Figure 3, the areas ΔA_i, with i=1,…,5, have been evaluated. The measurements were made at times: t_1=6, t_2=18, t_3=22, t_4=44, t_5=60 months. Starting by the ΔA_i evaluated and through a simple “data by data” linear of the loss interpolation, a first evolution over time process has been obtained as shown in Fig.6.

2.4 First observations and results

At this phase of the research, the following conclusions can be drawn:

- The stone panel shows a similar damage in the first and second courses; very low damages occur at the upper courses (Fig. 7).
- The damage corresponds to the highest level of the capillary rise surveyed by visual inspection.
- The damage is characterised, in the first and the second course, by: (*i*) a first phase of relatively fast loss of material (between 0 and 22 months); (*ii*) a steady state (between 22 and 44 months); (*iii*) a renewal of the decay process which started in July 1998, after 44 months.
- The damage is not deep but extended over a large surface.
- The damage is influenced by the bonding technique of the stones in the wall (stretchers or headers) (Fig. 8).

Since in fact the capillary rise in a stone – masonry takes place mostly through the joints due to the very different capillary rise coefficient of the two materials (in the case studied the coefficient has the values 0.27 $(kg/m^2)/s^{0.5}$ for the mortar and 0.006-0.007 $(kg/m^2)/s^{0.5}$ for the stone). Consequently, the most damaged areas are the ones adjacent to the joints; in fact the header stones show an apparent larger damage than the stretcher stones, referred in % to their area.

3. Theoretical approaches

The experimental data recorded have been the base on which the material deterioration was modelled in a probabilistic way.

3.1 The deterioration process as a stochastic process in the r.v. ℓ

The deterioration process of the stone masonry can be described through the parameter ℓ defined as the loss of material reached by the system at the time t^* of measurement. At every time t^*, the high randomness connected with the occurrence of the material decay in the natural environment brings to consider ℓ as a r.v. with a certain distribution of values (Fig. 9). Following this way, the deterioration process can be interpreted as a stochastic process of the r.v. ℓ. But the wall surface decay also depends on the time instant t^* in which the deterioration is recorded. Therefore, at each time t^* the loss ℓ (measured in mm^2) can be modelled with a probability density function (p.d.f.) $L(t^*,\ell)$ that results dependent on the time t^* = constant value (e.g.: t_1=6 months, t_2=18months and so on) and the r.v. ℓ. In order to model $L(t^*,\ell)$, at every time t^* a family of theoretical distributions has to be chosen. No doubt that, the choice of a distribution modelling a given phenomenon has to be connected to the physical aspects of the phenomenon itself and to the characteristics of the distribution function in its tail, where often no experimental data can be collected. This last aspect of the question can be investigated by analysing the behaviour of the immediate occurrence rate function $\phi_L(t^*,\ell)$ connected with the chosen distribution function:

$$\phi_L(t^*,\ell)dL = \Pr\{L < \ell \le L + dL \mid \ell \ge L\} \qquad (1)$$

On this subject more details are described in [7] and [10].

In the case proposed here, the recorded experimental data show a large dispersion around the average value of ℓ. This is probably due to the randomness connected to the decay mechanism in a real environment. However, the loss seems to be included in a certain range of values. Therefore, it seems correct to assume that, at a given time t^*, the probability of having a loss $(L < \ell \le L + dL)$ decreases as the value L (magnitude of the loss) increases. The assumed hypothesis as a satisfied (but not unique) physical interpretation of the decay process leads to model the loss ℓ at the time t^* with a Lognormal distribution (Fig. 9) as follows:

$$L(t^*, \ell) = \frac{1}{\ell \sqrt{(2\pi\alpha)}} \exp\left[-\frac{\{\log(\rho\,\ell)\}^2}{2\alpha} \right] \tag{2}$$

The estimation of the shape parameters α and ρ have been made through a computer code involving the maximum likelihood method. This modelling can be obtaining also through the function FMIN present in the MATLAB code.

This family of distributions presents an immediate occurrence rate function (1) decreasing as the value of L increases; this fact seems to respect the physical interpretation of the decay process previously proposed.

It is furthermore interesting to evaluate the probability for the system of reaching or exceeding a given damage threshold $\overline{L}$ over time. This probability can be seen as the dashed area over $\overline{L}$ as shown in Figure 10.

This area can be calculated by using the survive function $\Im_L(t^*, \ell) = 1 - F_L(t^*, \ell)$ where $F_L(t^*, \ell)$ is the cumulative distribution function of the p.d.f. (2).

The computation of $\Im_L(t^*, \ell)$ is possible with the use of any kind of computer code for numerical integration.

For different damage levels $\overline{L}$, the survive function has been evaluated for all the times t. The calculated values allow to plot an experimental "*fragility curve*" connected to each chosen damage level (see Fig. 11 in Section 4).

Following this approach the deterioration process can be treated as a reliability problem [6]. Indeed [11] the reliability *R*(*t*) concerns the performance of a system over time and it is defined as the probability that the system does not fail during the time *t.* Here this definition is extended and $\overline{R}(t)$ is assumed as the probability that a system exceeds a given significant damage threshold $\overline{L}$ in the time *t.* The random variable that is used to quantify reliability is $\overline{T}$ which is just the time to exceed damage $\overline{L}$. Thus, from this point of view, the reliability function is given by [11 and 12]:

$$\overline{R}(t) = \Pr(\overline{T} > t) = 1 - F_{\overline{T}}(t) \tag{3}$$

where $F_{\overline{T}}(t)$ is the distribution function for $\overline{T}$ and represent the theoretical modelling of the experimental fragility curves.

In order to model the experimental fragility curves and to evaluate $F_{\overline{T}}(t)$, a Weibull distribution has been chosen [5 and 10] as follows:

$$F_{\overline{T}}(t) = 1 - \exp\left[-(\rho t)^{\alpha}\right] \tag{4}$$

In fact this distribution seems to be a good interpretation of the physical phenomenon: the larger is the waiting time *t* to lose $\overline{L}$, the higher is the probability that the loss $\overline{L}$ will happen in the next (*t*+*dt*) time interval. Therefore distributions with the function $\phi_{\overline{T}}(t)$ increasing with *t* and tending to ∞ as $t \to \infty$ are needed. The Weibull distributions satisfy this requirement.

The fitting of the experimental fragility curves with the distribution (4) has been made through a computer code involving the least squares method.

3.2 The deterioration process as a stochastic process in the r.v. τ

The deterioration process can be seen as a material loss of performance. Each time the deterioration reaches a given level the material suffers a *"failure"*; therefore a loss of performance occurs [4]. The loss of performance can be defined as a change of service-state for the system; namely when the system suffers a failure it passes from the current service-state *i* to another state *k* characterised by a lower level of performance. Thus the deterioration process (failure process) may be defined as a *transition process* of the system through different service-states due to a discrete number of attacks in the time continuum, *t* [3].

Every transition depends on [4]:

- The magnitude of the attack (stress cycle);
- The system capacity to withstand this attack.

Both these parameters depend on a large number of time dependent r.v.; therefore it is correct to interpret the transition process as a stochastic process. In [7] it has been shown that a possible r.v. which can be assumed to describe a transition process is the service lifetime τ_i defined as: *"the waiting time spent by the material in the performance state i"*.

Under this point of view the reliability function R_{τ_i} can be defined as:

$$R_{\tau_i}(t,t_0) = \Pr\{\tau_i > t\} = 1 - F_{\tau_i}(t,t_0) \tag{5}$$

where t_0 represents the age of the material when the material enters the state *i* and F_{τ_i} the cumulative distribution function of the r.v., τ_i.

When F_{τ_i} is known, a stochastic dynamic process can be assumed to represent the material failure process. In [13] and [14] it has been shown that the semi-Markov Processes (s-MP) seem to suitably describe the material failure process. They allow to distinguish different states of the system with different waiting times and to take into account the age t_0 of the material when it is subjected to failure processes.

3.2.1 The semi-Markov approach: general remarks

The semi-Markov Processes (s-MP) are processes describing the behaviour of a dynamic system that changes its state at every transition; they appear to be suitable models to represent the failure process of a building material [3]. A s-MP is defined when the following quantities are known [15]:

a. Initial conditions: *initial state*, i.e. the state occupied by the system at the origin of time t=0, and the time t_0, *the time spent in the initial state* at the time t=0.

b. Probability density function (p.d.f.) $f_{ik}(t)$ of the waiting time τ_{ik}, i.e., the time spent in the state i if the next state is k: $f_{ik}(t)dt = \Pr\{t < \tau_{ik} \le t + dt\}$, where t = the time measured from the entrance in the state i.

c. Transition probability matrix, p_{ik}, defined as: $p_{ik} = \Pr\{\text{next state } k, \text{present state } i\}$.

Once the points *a, b* and *c,* are determined, the waiting time τ_i, introduced in 3.2, can be defined by the p.d.f.:

$$f_{\tau_i}(t) = \sum_k f_{ik}(t) p_{ik} \tag{6}$$

The probability that, at the time t, the system will occupy the state k, can be evaluated if the present state is i.

By these assumptions it is evident that in the semi-Markov hypothesis the failure prediction only depends on the transition probability p_{ik}, on the waiting time p.d.f. $f_{ik}(t)$, and on the initial conditions. The problem of the suitable choice of $f_{ik}(t)$, must now be solved.

As already said, in choosing $f_{ik}(t)$ attention is paid to the failure-rate function $\phi_{ik}(t)$ (fun. 1) and to the physical knowledge of the material deterioration phenomenon [7].

Since the deterioration is a renewal process, the larger is the waiting time τ_{ik}, spent by the system in the state i, the higher is the probability that the transition in the next state k can happen in the next (t+dt) time interval [5, 13]. Therefore, also in this case distributions with the function $\phi_{ik}(t)$ increasing with t and tending to ∞ as $t \to \infty$ are needed; the Weibull distributions present this behaviour.

3.3.2 The deterioration process as a renewal process

The experimental data collected show that the material failure process seems to renew itself each time the loss of surface material reaches a given level $\overline{L}$.

This suggests to model the material process of failure as a renewal process, [16] the simplest type of s-MP.

A renewal process is defined if:

- The service-states are defined;
- The waiting time τ_i spent by the system in each service-state i before moving to the following service-state k is modelled through appropriate p.d.f. $f_\tau(t)$.

In a renewal process $f_\tau(t)$ is the same for each τ_i. Only for the waiting time spent in the initial state the renewal process can present a different p.d.f.

Assuming the deterioration process to be a renewal process, from the experimental data it is possible to comment as follows:

1. For the service-states *0* of amplitude $\overline{L}$ mm^2.
   - Since the first transition occurs at 400mm^2 of damage, then $\overline{L}_0$ =400mm^2.
   - The initial *state 0* is characterised by a t_0=0, because the wall was a new wall when the test has begun.
2. For the service-states *i* (with *i*>0) of amplitude $\overline{L}$ mm^2.
   - Each transition after the first, occurs at every 200 mm^2 of material loss; therefore $\overline{L}_i$ =200mm^2.

On the base of the experimental data and of the previous points 1. and 2., it is possible to define:

- The transition probability $p_{i,k}$.

  The intervals chosen has guaranteed a sure transition between the different states; in this case $k = i + 1$ and the transition probability is: $p_{i,k}= 1$.
- The waiting time τ_{ik}. Precisely:

- The waiting time $\tau_{01} = \tau_1$ considered as the waiting time spent by the system in the initial state 0 before passing to the state 1.
- The waiting times representative of the successive transitions $\tau_{i,k} = \tau$, with $i > 0$ and $k = i + 1$.

4. Results and comments

The application of the two approaches proposed in 3.1 and 3.2 has shown some differences that will be pointed out in the following:

4.1 Fragility curves

The probabilistic approach proposed in 3.1 is able to model the deterioration in terms of probability to reach or exceed a given damage threshold $\overline{L}$ over time (Fig. 9 and 10). The assumption of the Lognormal distributions to model the experimental data has pointed out that the deterioration can change its behaviour over time with an increasing scattering (Fig. 9). This behaviour is probably due to the randomness connected with the realisation of the decay process in the real environment and of the characteristic of the panel (i.e.: presence of mortar joints, prevailing of headers along the profile, profile position close to the mortar-stone interface, etc). The modelling has been obtained through a computer code involving the maximum likelihood method. The logarithm of the maximum likelihood function and the values of the other statistical test performed, associated to the physical knowledge on the deterioration, seem to well support the choice made.

The experimental fragility curves, obtained by computing the equation (3), are plotted in Figure 11. The fitting is obtained through a computer code involving the least square method. Also in this case the values given by the least square method and the values of the other statistical test performed, associated to the physical knowledge on the deterioration and the statistical knowledge, support the choice made.

From Figure 11 it is evident that the probability of exceeding a given damage $\overline{L}$ in a short time is lower if $\overline{L}$>600mm^2 and higher if $\overline{L}$<400mm^2. In fact, the plot shows a high probability that a small delamination ($\overline{L}$=200-400mm^2) happens in *t*=20months from the initial time. Instead the probability to have a higher loss ($\overline{L}$=800mm^2) increases only for *t*>>120months after the initial time.

The approach proposed in 3.1 can point out the failures with higher or lower probability of occurrence in the given time *t*. The fitting shown by Fig. 11 is satisfactory; nevertheless a small sample was used. Therefore, in order to interpret these results much caution is needed. This means that, when the application of this approach is simple, in order to have significant results the time of monitoring and the data recorded have to be very long.

4.2 The semi-Markov approach

The probabilistic approach proposed in 3.2 is able to model the deterioration process as a transition process. The application of the s-MP needs the definition of some service-states through which the system passes during its deterioration process (each state is characteristic of a given damage level). The choice of the service-states is not simple. Being arbitrary it can compromise the interpretation of the analysed process. In fact this choice on the type of failure, on the physical aspect of the investigated phenomenon, but also on which loss is defined as damage: a very thin delamination or a thick one. In [13 and 14] the authors have shown that the salt decay process of the masonry components (stones, bricks, and mortars) can be modelled as a renewal process. Here the choice of the state had the aim of verifying whether the decay process of the masonry as a composite material is still a renewal processor not. The choice has not been so difficult.

If the experimental data are considered, the deterioration process shows a bi-modal behaviour. Since the masonry has been assumed as a composite material, the bi-modal behaviour could be connected with the two different deterioration process of stone and mortar.

To capture the bi-modality of the process a mixture of two Weibull densities of the type:

$$f_{\tau_\bullet}(t) = \alpha\rho(\rho t)^{\alpha-1}\exp\left[-(\rho t)^{\alpha}\right] \qquad \text{(with } \tau_\bullet = \tau_1 \text{ or } \tau_\bullet = \tau) \tag{7}$$

have been adopted in (8):

$$f_\tau(t) = pf_1(t) + (1-p)f_2(t) \tag{8}$$

where: $f_1(t)$ is representative of a short term damage; $f_2(t)$ is representative of a long term damage; while p and $(1-p)$, are, respectively the probability of a close transition (short term damage) and of a delay transition (long term damage).

The results obtained by the application of the semi-Markov approach shows a different behaviour of the waiting time τ_1 describing the first transition (reaching the 1st threshold $\overline{L}_1$=400mm^2), from the behaviour of the waiting times τ, describing the following transitions.

Through a computer code, involving the maximum likelihood method, the modelling of the experimental data has been made and the shape parameters, describing the Weibull distributions, have been estimated. Through significance test included in the code, the reliability of the fitting has been proved. The fitting of the experimental data is plotted in Figure 12 and 13.

The computer code used was implemented to study each probabilistic problem modelling through classic distributions (LogNormal, Weibull, Gamma, etc.) and mixture of them. The frame of it consists in a Fortran code re-calling different functions of IMSL Libraries for UNIX [16].

Precisely, the parameter estimation has been made using the function minimisation with Rosenbrock's method. But, as said before, problems of non-linear minimisation can be solved also through the function FMIN present in MATLAB code.

The results obtained seem to confirm the hypothesis that the material failure process is a renewal process. Since the p.d.f. describing the waiting times of the first transition: τ_1 has a different shape with respect to the p.d.f. modelling the waiting times at the successive transitions: τ, the material failure process seems to follow a *modified renewal process* [17].

As commented in 3.2 the s-M approach is able to take into account the time t_0 elapsed from the construction of the building (or the surface treatment) and the precise time when the analysis of its deterioration starts. Therefore, no information is lost.

Besides, if the process modelled is a renewal process the time of monitoring can be reduced because the process renews itself at every $\overline{L}$ of material lost and only the knowledge of the waiting times concerning the first two transitions is needed.

4.3 Maintenance planning using the probabilistic approaches proposed: some remarks

The approaches proposed to model the deterioration process are able to give information, in probabilistic terms, on the occurrence time of a given damage level $\overline{L}$ to the studied system.

In fact, with the computing of the fragility curves the probability to exceed a given damage level $\overline{L}$ at every time *t* is defined, so that the probability of occurrence of different damage levels at the time *t**, can be easily evaluated.

In the case of a renewal process the prediction, in probabilistic terms, can refer to the prediction of:

- The occurrence time of the r^{th} renewal;
- The number of renewals in a certain time *t**.

Since a renewal happens every time the damage threshold $\overline{L}$ is reached, this approach allows to make predictions also on:

- The occurrence time of the damage level L_r connected with the r^{th} renewal;
- The damage level reached with the renewals occurred in the time *t**.

The knowledge of the probability of occurrence of a given damage level $\overline{L}$ at the time *t*, means that it is possible to plan maintenance strategies known in terms of execution, durability and effectiveness. As an example, the time *t**, connected with the probability of exceeding $\overline{L}$, can be assumed as the right moment to operate a maintenance action on the system. This action will lead the system to a better service-state than the one corresponding to the time t*, thought it is usually unable to lead the system to the original (first) service-state. Therefore, it is possible that a certain damage remains. The analysis carried at the further level has to take into account this damage, so the probability to exceed $\bar{L}$ would be reached in a time $\bar{t} < t^*$ and the time interval between the maintenance actions could not be constant.

The use of the proposed approach allows the investigation of this eventuality.

Following the same way, questions concerning the durability and the effectiveness of maintenance and repair actions, as the surface treatment effectiveness, can be dealt with.

5. Conclusions

During their service life, masonry subjected to an aggressive environment may suffer degradation. The great randomness connected with the occurrence of critical attacks by salt crystallisation suggests approaching the deterioration process of these materials from a probabilistic point of view. The material deterioration process has been approached as a reliability problem where:

i) The reliability function $R_{\bar{T}}$ has been defined as a function of the r.v. ℓ = loss of surface material. The failure process is seen as the probability of the system to exceed a given damage level $\bar{L}$. The fragility curves obtained allow defining the exceedence probability over time connected with each $\bar{L}$ chosen.

ii) The failure process is assumed to be a *transition process*. To model it the s-MP have been proposed. In order to describe the time dependent reliability function R_{τ_i}, the r.v. τ_i has been defined, where τ_i = waiting time spent by the system in a given service-state i before passing in a successive service-state.

From the experimental investigation the failure process seems to renew itself at every $\bar{L}$. By modelling the deterioration process as a renewal process it is possible to make prevision: on the time $\bar{t}$ needed at the system to reach a given damage level L and on the damage level L^* reached by the system in a given time t.

A comparison between the two approaches has been made. It has been pointed out how the success depends on the type of the studied problem and how is important to have the knowledge of the physical aspects of the analysed phenomenon, in order to correctly model it. The comparison has shown how both the approaches are able to predict, in probabilistic terms, the magnitude of the expected damage over time and the occurrence time for a given damage level. This important information allows to appropriately plan of the maintenance and repair of the wall surface.

6. References

1. Binda, L., Baronio, G., Ferrieri E.D. and Rocca, P., 'Full scale models for the calibration of laboratory ageing test', Proc. of 7DBMC, 7th International Conference on Durability of Building Materials and Components, Stockholm, Sweden, (E&FN SPON, London, ISBN 0-419-20690-6, 1996) 968-978.
2. Binda, L., Baronio, G., Lubelli B. and Rocca P., 'Effectiveness of surface treatments of stone and brick masonry: proposal and calibration of on site control techniques', Proc. of 8DCMC, 8th International Conference on Durability of Building Materials and Components, Vancouver, Canada, **1** (1999) 538-549.
3. Guagenti, E., Molina, C., Binda, L. and Garavaglia, E., 'Predictable models in earthquake engineering and in materials durability', Proc. 4th Symp. ASMDA4, INRA*,* Nancy, France, **1** (1988) 79-97.
4. Sarja, A., 'Towards practical durability design of concrete structures', Proc. of 7DBMC, 7th International Conference on Durability of Building Materials and Components, Stockholm, Sweden, E&FN SPON, London, **2**, (1996) 1238-1247.
5. Bekker, P.C.F., 'Durability testing of masonry: statistical models and methods', *Masonry International,* **13**(1) (1999) 32-38.
6. Binda, L., Garavaglia, E. and Molina, C., 'Physical and mathematical modelling of masonry deterioration due to salt crystallisation', Proc. of 8DCMC, 8th International Conference on Durability of Building Materials and Components, Vancouver, Canada, M. A. Lacasse, D. J. Vanier Editors, NRC-CNRC, Ottawa, Vol. I, pp. 527-537, ISBN 0 660 17737 4 (1999).
7. Binda, L. and Molina, C., 'Building Materials Durability Semi-Markov Approach', *Journal of Materials in Civil Engineering*, ASCE, U.S.A., **2**(4), (1990) 223–239.
8. Binda, L., Baronio, G. and Squarcina T., 'Evaluation of the durability of bricks and stones and of preservation treatments, 7th Int. Congress of Deterioration and Conservation of Stone, Lisbon, **2**,(1992) 753-761.
9. Berra, M., Fatticcioni, A., Binda, L. and Squarcina, T., 'Laboratory and in-situ measurements procedure of the decay of masonry surfaces', 6th Int. Conf. on Durability of Building, Materials and Components, Omiya, **2**, (1993) 834-843.

10. Garavaglia, E., Lubelli, B. and Binda, L., ‘Service life modelling of stone and bricks masonry walls subject to salt decay’, Proc. of ILCDES 2000, Integrated Life-Cycle Design of Materials and Structures, Helsinki, Finland, A. Sarja Ed., RILEM/CIB/ISO, Pro 14,Technical Research Center of Finland (VTT), Helsinki, ISBN 951-758-408-3, **1** (2000) 367- 371,

11. Evans, D.H., ‘Probability and its Applications for Engineers’, Marcel Dekker, Inc., New York, NJ, USA. (1992).

12. Melchers, R.E., ‘Structural reliability - analysis and prediction’, Ellis Horwood LTD, Chichester, West Sussex, England, ISBN 0-85312-930-4. (1987).

13. Molina, C, Garavaglia, E., Bekker, P. and Binda, L., ‘A Service Life Prediction Model for Masonry Based on Accelerated Testing and Weibull Interpreted Testing Results’, Proc. of 7DBMC, 7th International Conference on Durability of Building Materials and Components, Stockholm, Sweden, E&FN SPON, London, ISBN 0-419-20690-6, **1**, (1996) 75-84.

14. Garavaglia, E., Binda, L. and Lubelli, B., ‘Masonry wall deterioration problem: A possible probabilistic approach’, Proc. of ICASP8, 8th International Conference on Application of Statistic and Probability, Sydney, Australia, Melchers & Steward Eds, A.A. Balkema, Rotterdam, ISBN 90 5809 087 6, **1**., (1999) 337-343.

15. Howard, R.A., ‘Dynamic probabilistic system’, John Wiley and Sons, (New York, N.Y. 1971)

16. IMSL, Numerical Libraries, Math/Library Vol. 1 e 2, FORTRAN and C application development tools from Visual Numerics Inc.

17. Cox, D.R., ‘Renewal Theory’, Methuen LTD, London, U. K. (1962).

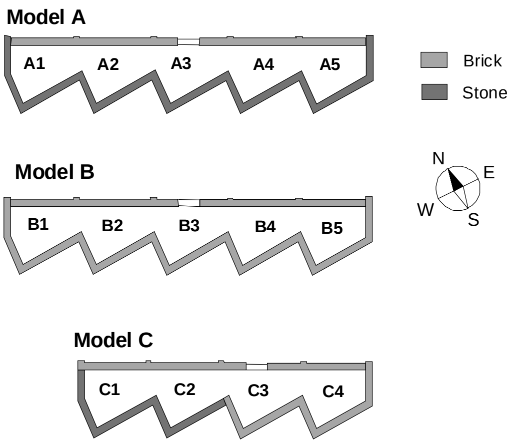
Model A
A1
A2
A3
A4
A5
Brick
Stone
Model B
B1
B2
B3
B4
B5
N
E
W
S
Model C
C1
C2
C3
C4

Fig. 1a

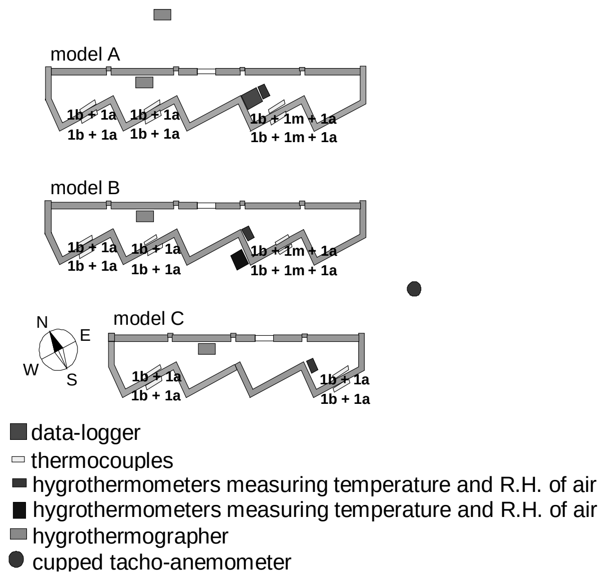
model A
1b + 1a
1b + 1a
1b + 1a
1b + 1a
1b + 1m + 1a
1b + 1m + 1a
model B
1b + 1a
1b + 1a
1b + 1a
1b + 1a
1b + 1m + 1a
1b + 1m + 1a
N
E
W
S
model C
1b + 1a
1b + 1a
1b + 1a
1b + 1a
data-logger
thermocouples
hygrothermometers measuring temperature and R.H. of air
hygrothermometers measuring temperature and R.H. of air
hygrothermographer
cupped tacho-anemometer

Fig.2a

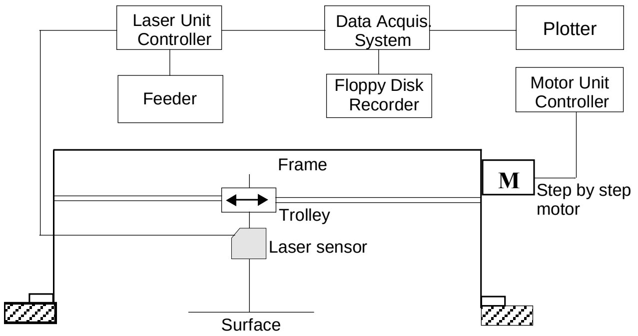
Laser Unit Controller
Data Acquis. System
Plotter
Feeder
Floppy Disk Recorder
Motor Unit Controller
Frame
M
Step by step motor
Trolley
Laser sensor
Surface

Fig. 2c

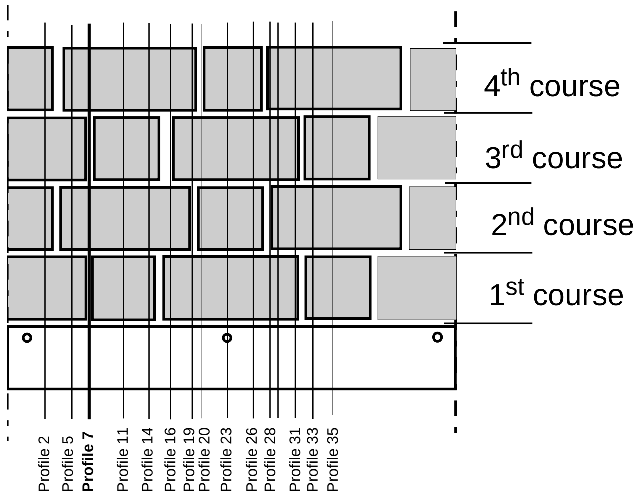
4th course
3rd course
2nd course
1st course
Profile 2
Profile 5
Profile 7
Profile 11
Profile 14
Profile 16
Profile 19
Profile 20
Profile 23
Profile 26
Profile 28
Profile 31
Profile 33
Profile 35

Fig. 3

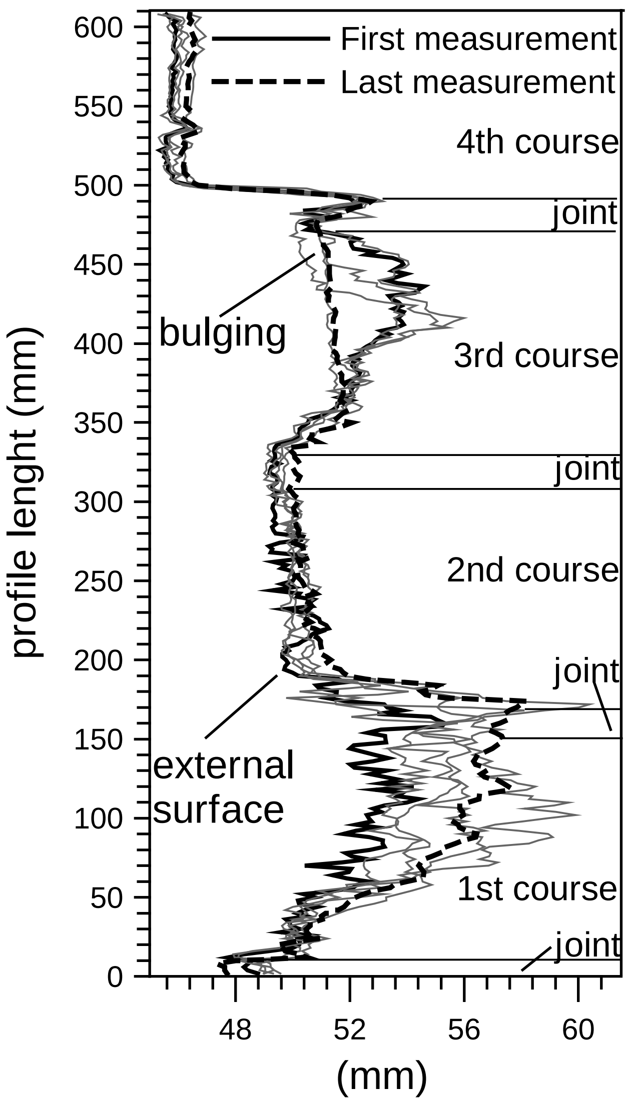
First measurement
Last measurement
4th course
joint
bulging
3rd course
joint
2nd course
joint
external
surface
1st course
joint
profile lenght (mm)
(mm)
0
50
100
150
200
250
300
350
400
450
500
550
600
48
52
56
60

Fig. 4a

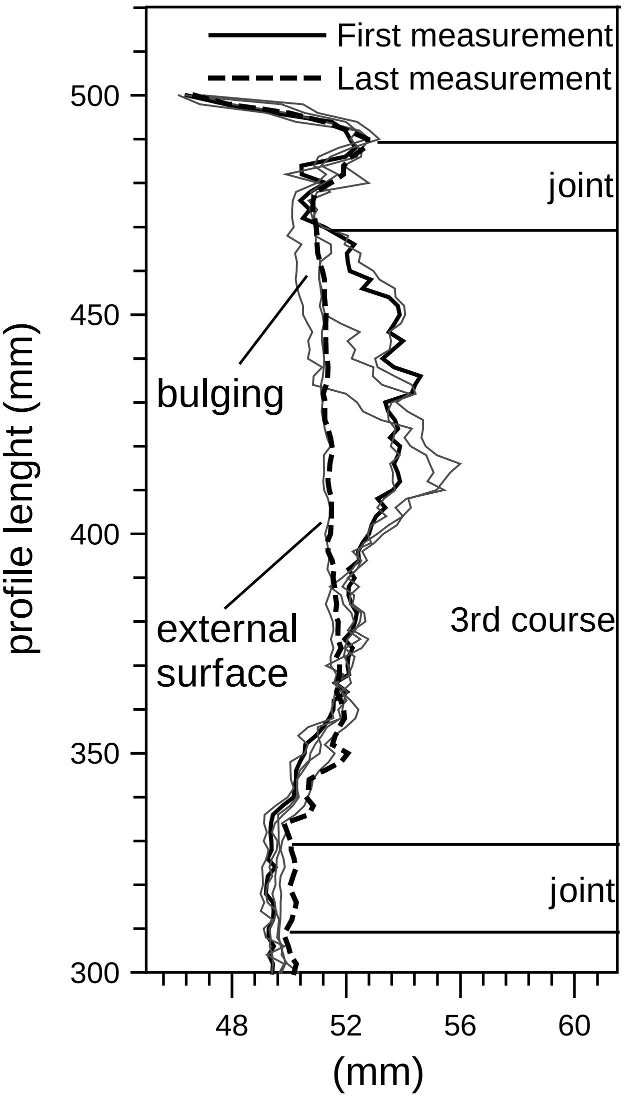
First measurement
Last measurement
joint
bulging
external surface
3rd course
joint
profile lenght (mm)
(mm)
500
450
400
350
300
48
52
56
60

Fig.4b

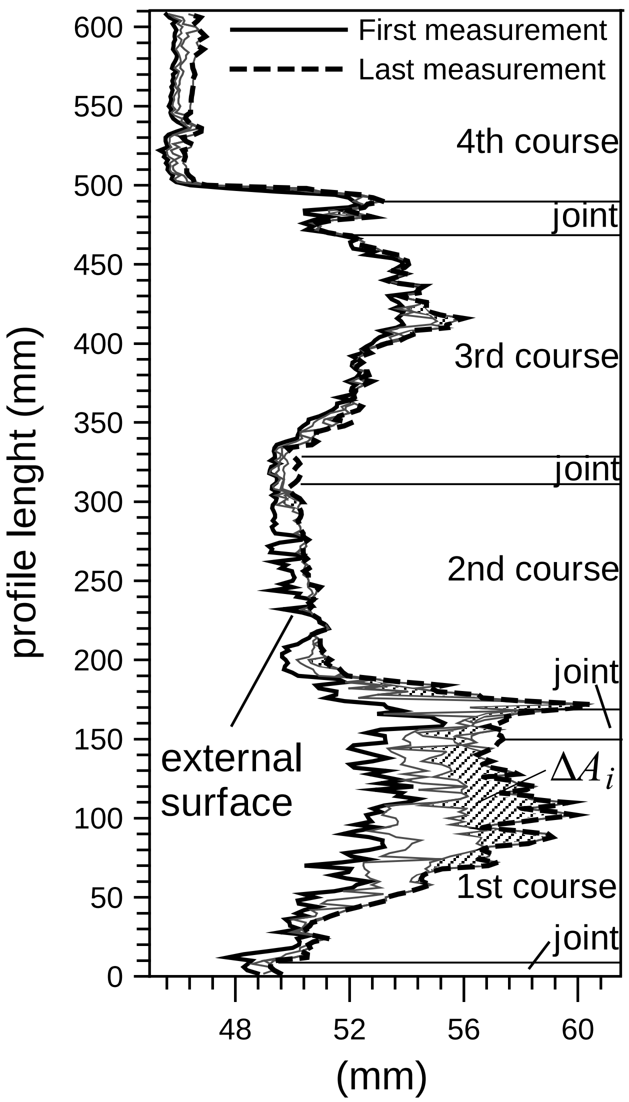
First measurement
Last measurement
4th course
joint
3rd course
joint
2nd course
joint
external surface
ΔA_i
1st course
joint
profile lenght (mm)
(mm)
0
50
100
150
200
250
300
350
400
450
500
550
600
48
52
56
60

Fig. 5

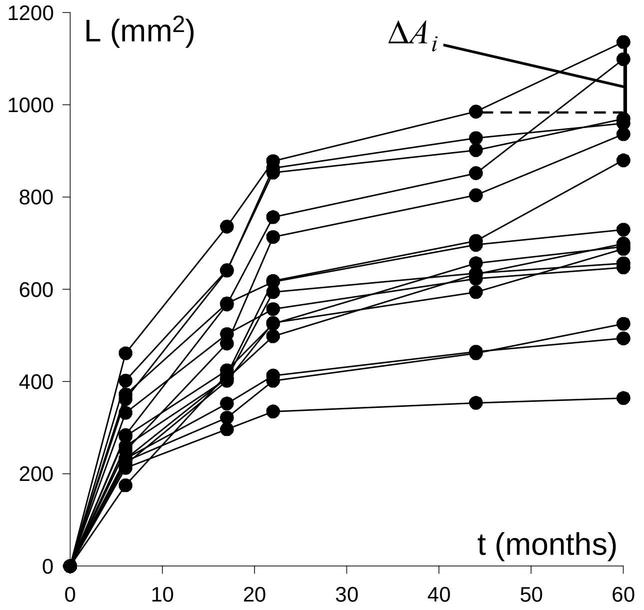
L (mm2)
ΔAi
t (months)
1200
1000
800
600
400
200
0
0
10
20
30
40
50
60

Fig. 6

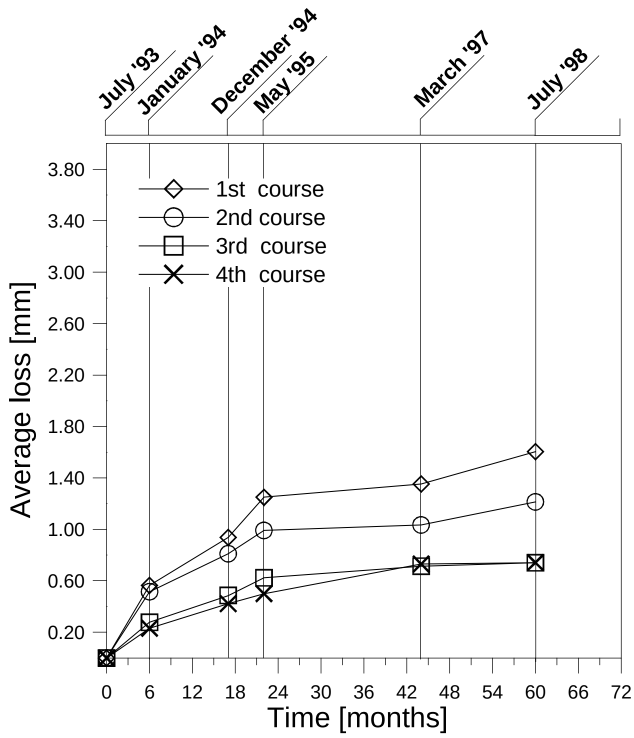
July '93
January '94
December '94
May '95
March '97
July '98
1st course
2nd course
3rd course
4th course
Average loss [mm]
Time [months]
3.80
3.40
3.00
2.60
2.20
1.80
1.40
1.00
0.60
0.20
0
6
12
18
24
30
36
42
48
54
60
66
72

Fig. 7

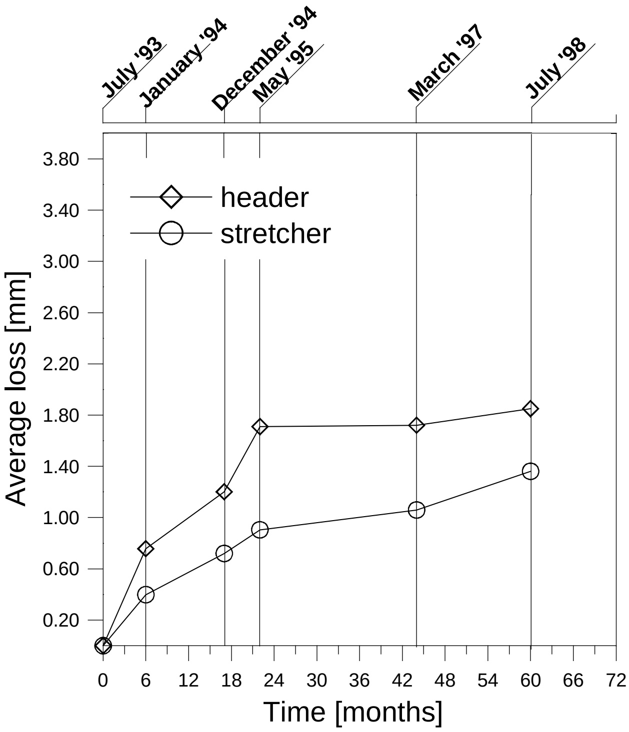
July '93
January '94
December '94
May '95
March '97
July '98
header
stretcher
Average loss [mm]
3.80
3.40
3.00
2.60
2.20
1.80
1.40
1.00
0.60
0.20
0 6 12 18 24 30 36 42 48 54 60 66 72
Time [months]

Fig. 8

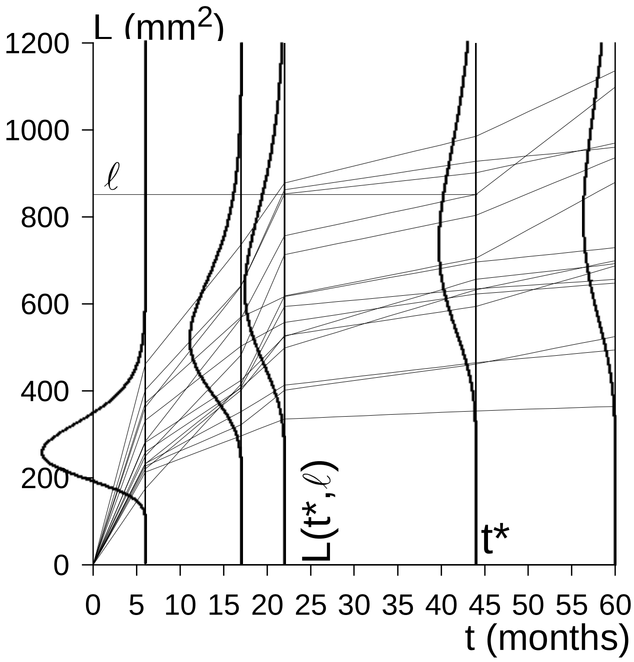
L (mm^2)
1200
1000
800
600
400
200
0
ℓ
L(t*,ℓ)
t*
0 5 10 15 20 25 30 35 40 45 50 55 60
t (months)

Fig. 9

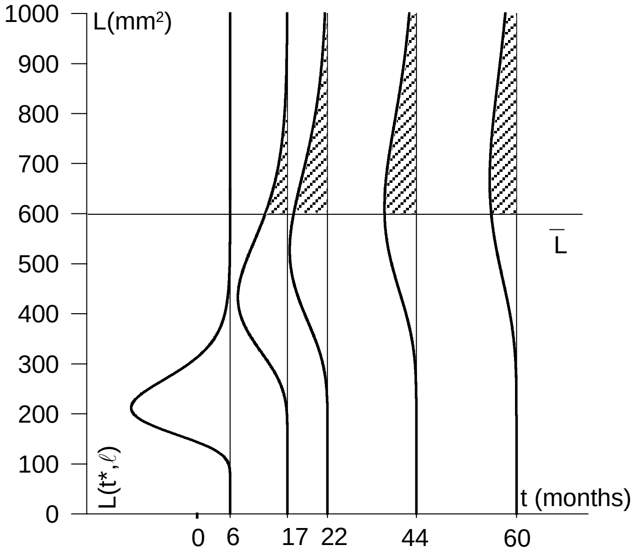
1000
900
800
700
600
500
400
300
200
100
0
L(mm²)
L(t*,ℓ)
t (months)
0
6
17
22
44
60
L

Fig. 10

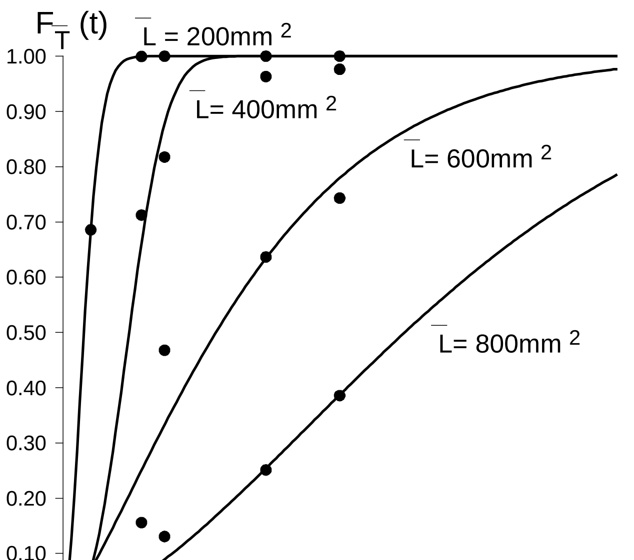
F_T (t)
L = 200mm 2
L= 400mm 2
L= 600mm 2
L= 800mm 2
1.00
0.90
0.80
0.70
0.60
0.50
0.40
0.30
0.20
0.10
0.00
t (months)
0
10
20
30
40
50
60
70
80
90
100
110
120

Fig. 11

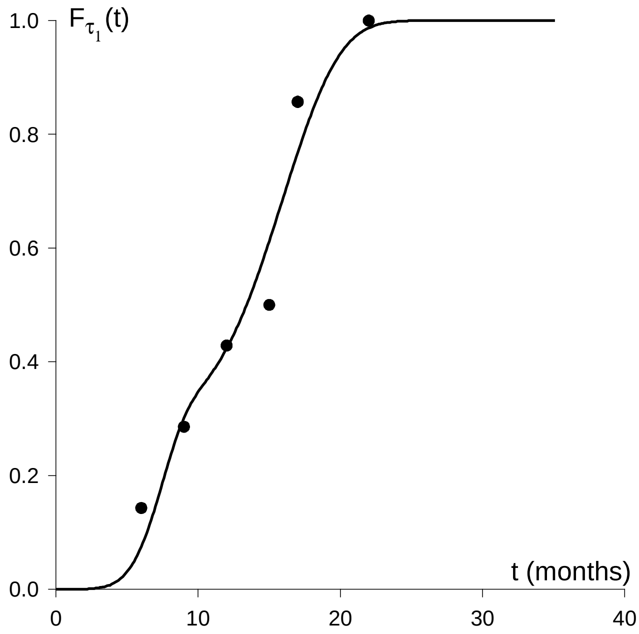
$F_{\tau_1}(t)$
1.0
0.8
0.6
0.4
0.2
0.0
t (months)
0
10
20
30
40

Fig. 12

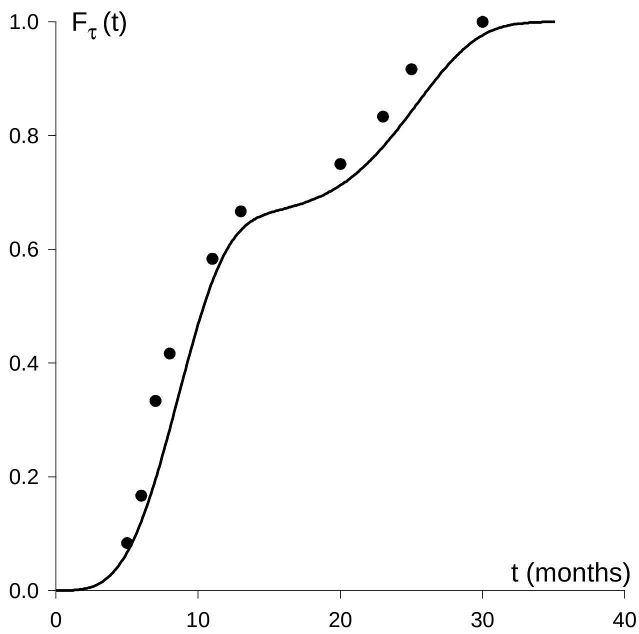
$F_{\tau}(t)$
1.0
0.8
0.6
0.4
0.2
0.0
t (months)
0
10
20
30
40

Fig. 13